Proceedings of ITC18, 2008

Simultaneous measurement of electron and ion temperatures with helium-like argon spectrum

Motoshi GOTO and Shigeru MORITA

National Institute for Fusion Science, Toki 509-5292, Japan

The helium-like argon spectrum is measured for the plasma in the Large Helical Device (LHD). The electron temperature T_e derived from the intensity ratio of the resonance line ($1s^2\,{}^1S_0 - 1s2p\,{}^1P_1$) to a dielectronic satellite line ($1s^22p\,{}^2P_{1/2} - 1s2p^2\,{}^2D_{3/2}$) is consistent with the central T_e measured with the Thomson scattering method when the electron density n_e has a peaked profile. The ion temperature T_i is simultaneously determined from the Doppler broadening width of the resonance line and the establishment of thermal equipartition between electrons and ions, i.e., $T_i = T_e$, due to the increase of n_e is experimentally confirmed.

Keywords: X-ray spectroscopy, helium-like argon, dielectronic satellite line, electron temperature measurement, ion temperature measurement

DOI:

1 Introduction

The x-ray spectroscopy has played an important role to measure the central ion temperature T_i in the fusion experiments. In LHD (the Large Helical Device), the temporal development of T_i is measured for every discharge from the Doppler broadening of the helium-like resonance line of argon, i.e., Ar XVII $1s^2\,{}^1S_0 - 1s2p\,{}^1P_1$ [1].

Besides the ion temperature measurement, the helium-like spectrum has found various uses for the plasma diagnostics in the core region. The helium-like spectrum here means a group of several emission lines corresponding to the transitions from $n = 2$ levels, where n is the principal quantum number, to the ground state of helium-like ion and numerous satellite lines of lithium-like ion which appear in the same wavelength range as the former.

The measurement of the electron temperature T_e with the intensity ratio of the dielectronic satellite line to the resonance line is an example of the applications of the helium-like spectrum [2, 3]. This method utilizes the different T_e-dependence of the rate coefficients for the electron impact excitation and dielectronic capture processes. The reliability of the derived parameter naturally depends on the accuracy of the atomic data.

Many efforts have been made to improve the theoretical calculation method for the required atomic data. In TEXTOR the measured spectra were compared with synthetic ones based on the newly calculated data and a comprehensive consistency between them was obtained [5]. Similar comparison was also made in NSTX [3], where it was demonstrated that the temporal behaviour of the derived electron temperature was consistent with the result of the Thomson scattering measurement.

In this paper, the temporal behaviors of T_i and T_e are simultaneously derived from the helium-like argon spectra taken for LHD and their consistency with the change of the background plasma condition is examined.

author's e-mail: goto@nifs.ac.jp

2 Experimental setup

The measurement is made for a discharge with the magnetic configuration of $R_{ax} = 3.8$ m and $B_{ax} = 2.539$ T, where R_{ax} and B_{ax} are the major radius of the magnetic axis and the magnetic field strength on the magnetic axis, respectively. The temporal development of the discharge is shown in Fig. 1. The plasma is started up with the electron cyclotron heating (ECH), and is sustained with three neutral beams (NBI). The argon gas-puff is provided at $t = 0.3$ s with the 10 ms pulse width. Eight hydrogen pellets are sequentially injected with a 40 ms interval from $t = 0.7$ s.

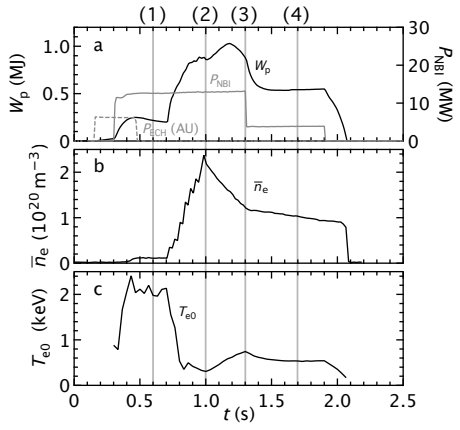

Fig. 1 Several parameters for the discharge analyzed here (#69260): (a) the ECH and NBI powers, P_{ECH} and P_{NBI}, respectively, and the stored energy W_p, (b) the line-averaged electron density $\bar{n}_e$, and (c) the central T_e by Thomson scattering method. T_e and n_e profiles at the timings (1)–(4) are shown in Fig. 6.

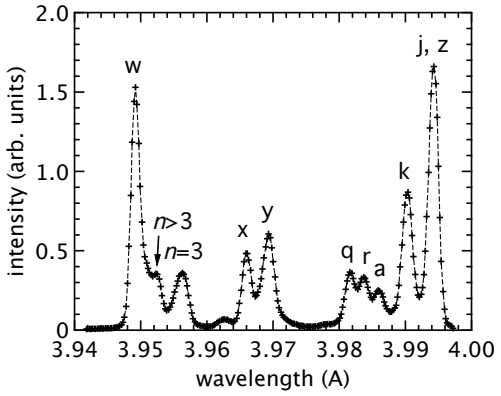

Fig. 2 Example of the measured spectrum made up of the data from two identical LHD discharges #69258 and #69260. The data are summed over from $t = 1.5$ s to $t = 1.7$ s. The line notation follows Ref. [4].

The line-averaged electron density $\overline{n}_e$ is derived from the radial profile data measured with the Thomson scattering method but the interferometer data in the initial low density phase are used to calibrate the absolute value. It is clearly seen that $\overline{n}_e$ stepwise increases synchronizing with each pellet injection. The central electron temperature T_e is immediately lowered after the pellet injection is started.

The helium-like argon spectrum is measured with a Johann-type crystal spectrometer which is basically the same as that described in detail in Ref. [1] but the radius of curvature of the quartz crystal (2020) has been changed from 3000 mm to 1500 mm. This modification aims at observing a wider wavelength range in a single measurement. The lattice spacing of the crystal is 4.2554 Å. The Bragg angle and the wavelength dispersion at $\lambda = 3.9492$ Å, which is the wavelength of the helium-like argon resonance line ($1s^2\,{}^1S_0 - 1s2p\,{}^1P_1$), are 68.1320 degree and 874.049 mm/Å, respectively.

A charge coupled device (CCD) is used as the detector. The detection area consists of 1024 pixels (in the direction of wavelength dispersion) times 256 pixels and the pixel size is $26 \times 26\,\mu m^2$. The spectra is obtained every 4 ms.

Figure 2 shows an example of the measured spectra for the discharge in Fig. 1. Here, the data are summed over the time period from $t = 1.5$ s and $t = 1.7$ s. The notation of lines follows Gabriel's definition [4]. The w, x, y, and z lines correspond to the transitions $1s^2 - 1s2l$ of helium-like ion and other lines indicated in Fig. 2 to the representative transitions of doubly excited lithium-like ion, i.e., $1s^2 2l' - 1s2l2l'$. The two groups of lines designated as $n = 3$ and $n > 3$ correspond to the transitions $1s^2 nl' - 1s2lnl'$ with $n \geq 3$.

It should be noted here that the detector size is insufficient to get the entire spectrum in Fig. 2 with a single discharge. The spectrum in Fig. 2 is made up of the data from successive two discharges which are almost identical. In the first measurement the wavelength range involving the w to y lines is observed and for the subsequent discharge the detector position is shifted so that the wavelength range involving the y to z lines is covered. The amplitude of the data taken in the second measurement is normalized to that of the first measurement at the y line which is involved in the both measurements. Here, the signal count is summed every eight channels and is represented by a single point in Fig. 2.

3 Model calculation

Here, we focus on the line intensity ratio of the k and w lines which is known to have a strong T_e-dependence [3]. Figure 3 shows a part of the energy level diagram of argon ion relevant to those lines. The upper level of the w

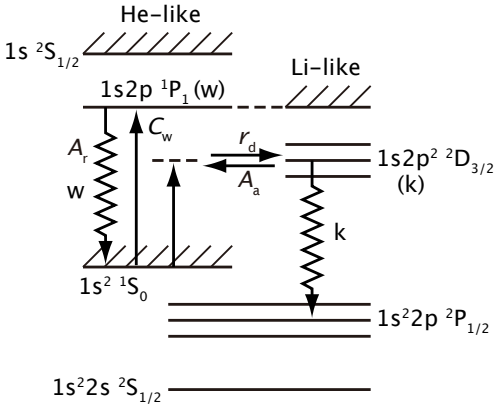

Fig. 3 Schematic energy level diagram relevant to the w and k lines of helium-like and lithium-like ions.

line $1s2p^1P_1$, which is also denoted by w here, is considered to be in corona equilibrium, namely, its population is determined so that the excitation from the ground state $1s^2{}^1S_0$ and the radiative deexcitation to the ground state are balanced. Under corona equilibrium the populations of the ground state and the w level, n_g and n_w, respectively, should satisfy the equation

$$C_w n_g n_e = A_w n_w, \tag{1}$$

where C_w is the excitation rate coefficient due to electron impact from the ground state to the w level, A_w is the spontaneous radiative transition probability from the w level to the ground state, and n_e is the electron density. The right-hand-side of Eq. (1) is nothing but the intensity or the photon emission rate of the w line.

The upper level of the k line, which is also denoted by k here, is the doubly excited state of lithium-like ion $1s2p^2{}^2D_{3/2}$. The k level is mainly populated through the dielectronic capture by the ground state helium-like ion which is indicated with an arrow labeled as r_d in Fig. 3. The dominant population outflow processes are the autoionization and radiative decay to the singly excited level

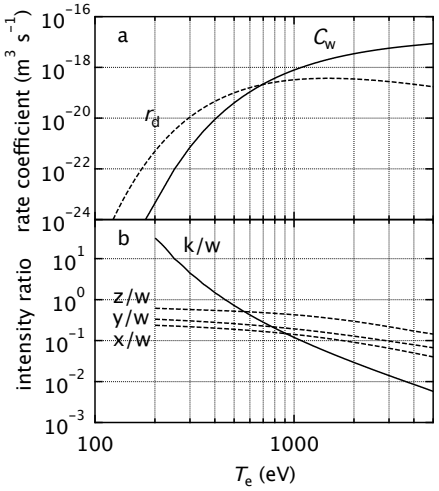

Fig. 4 T_e-dependence of the rate coefficients C_w and r_d (a) and intensity ratios between helium-like lines k/w, x/w, y/w, and z/w (b).

$1s^2 2p^2 P_{1/2}$. The latter process is called the stabilizing transition. The k level population, n_k, is determined so that these processes are balanced as

$$n_g n_e r_d = n_k (A_r + A_a), \tag{2}$$

where r_d is the rate coefficient of the dielectronic capture, and A_r and A_a are the probability for the stabilizing transition and the autoionization, respectively.

Since the dielectronic capture is the reverse process of the autoionization, r_d and A_a should satisfy the detailed balance equation under thermodynamic equilibrium as

$$\left[n_g n_e r_d = n_k A_a \right]_E , \tag{3}$$

where $[\cdots]_E$ indicates the condition of thermodynamic equilibrium. The rate coefficient r_d is expressed as

$$r_d = \left[\frac{n_k}{n_g n_e} \right]_E A_a = Z_k A_a, \tag{4}$$

where

$$Z_k = \frac{g_k}{2 g_g} \left(\frac{h^2}{2\pi m k T_e} \right)^{3/2} \exp\left(-\frac{\chi_{gk}}{k T_e} \right) \tag{5}$$

is the Saha-Boltzmann coefficient. Here, g_g and g_k are the statistical weights of the helium-like ground state and the level k, respectively, χ_{gk} is the energy level difference between these levels, and h, m, and k are the Planck constant, electron mass, and Boltzmann constant, respectively. Substituting Eq. (4) into Eq. (2) one obtains

$$n_k = \frac{A_a}{A_r + A_a} Z_k n_e n_g. \tag{6}$$

The intensity of the k line is obtained as $n_k A_r$.

The intensity ratio of the k to w lines I_k/I_w is now expressed as

$$\frac{I_k}{I_w} = \frac{A_r A_a Z_k}{C_w (A_r + A_a)}. \tag{7}$$

The T_e-dependence of C_w and r_d are shown in Fig. 4 (a) and I_k/I_w is shown in Fig. 4 (b). The values C_w, A_r, and A_a are taken from Ref. [5]. The strong T_e-dependence of I_k/I_w stems from the different T_e-dependence of C_w and r_d. Intensities of other helium-like ion lines, x, y, and z, can be obtained from a relation similar to Eq. (1). Figure 4 also shows the intensity ratios of x, y, and z lines to the w line. The advantage of use of the k/w ratio in comparison with other line ratios for the T_e measurement is clearly observed.

4 Results and discussion

The intensities of the w and k lines are derived from the measured spectra: each line profile is fitted with a Gaussian function and its intensity is obtained as the integral of the function.

The temporal development of the k to w line ratio is shown in Fig. 5. The electron temperature is readily determined from the calculation result in Fig. 4. The result is shown in Fig. 5. In Fig. 5 the central electron temperature measured with the Thomson scattering method is also shown. Before pellet injection ($t < 0.7$ s) the discrepancy between two results is large. After starting the pellet injection the both values immediately coincide with each other.

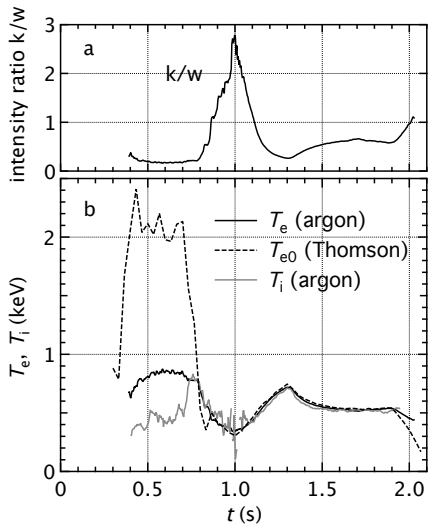

Fig. 5 Measured intensity ratio of the k and w lines for the discharge in Fig. 1 (a) and T_e derived from the k/w ratio, central T_e by Thomson scattering, and T_i from Doppler broadening of the w line (b).

The disagreement between the two measurements in the early time period can be understood from the fact that the present result is based on a line-integral measurement. Figure 6 shows the radial profiles of T_e and n_e measured at the timings indicated in Figs. 1. In the initial low density phase the T_e has a peaked profile while n_e profile is hollow. Roughly speaking, the line intensity is proportional to the product of n_i and n_e, here n_i stands for the helium-like ion

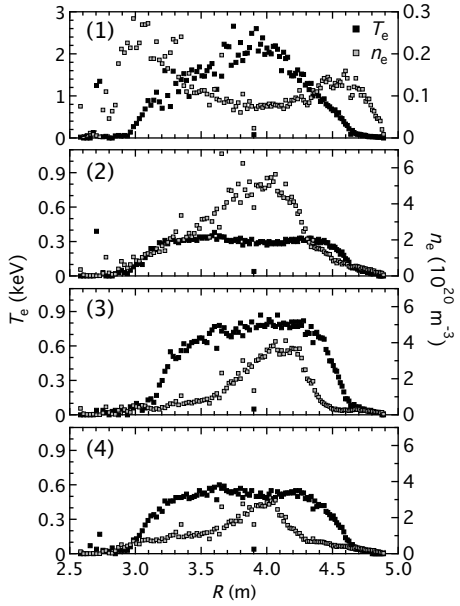

Fig. 6 Radial profiles of T_e and n_e measured with the Thomson scattering method at different four stages ((1)–(4)) of the discharge in Fig. 1.

density. Although the density profile of helium-like ion is probably peaked at the center, the line intensities could have a broad profile due to the relatively high n_e in the edge region. Therefore, the contribution of the edge emission in the observed line intensity might be so large that the apparent T_e is lowered.

After starting the pellet injection the T_e profile becomes rather flat and n_e is peaked at the center. Such characteristics, i.e., peaked n_e and flat T_e profiles, are sustained until the end of discharge although the highest values are dynamically changed. Since T_e profile is flat in this time period, the value derived with the present method can be regarded as that at the plasma center. As seen in Figure 5, the present result shows a good consistency with the Thomson's data, and the reliability of the present method is demonstrated.

We next consider the line profile for the T_i measurement. The ion temperature can be, in principle, derived from the Doppler broadening profile of an appropriate emission line. However, since the measured line profile is generally a convolution of the instrumental profile and the Doppler profile, deconvolution of the measured line profile into two profile components is necessary to determine T_i.

The instrumental profile, which is here approximated with a Gaussian function and represented by its width w_{inst}, is evaluated as follows. When the density is so high that equilibrium between the electron and ion temperatures, namely, $T_i = T_e$, can be assumed, the Doppler (Gaussian) width w_D is estimated from the measured T_e. Since the measured line width w_{obs} has a relationship with w_{inst} and w_D as

$$w_{obs}^2 = w_D^2 + w_{inst}^2, \tag{8}$$

w_{inst} is derived. Here, w_{inst} for the w line at $t = 1.7$ s is determined and thereby T_i in the entire discharge time is derived. The relation among w_{obs}, w_{inst}, and w_D at $t = 1.7$ s is shown in Fig. 7 and the eventually derived T_i is shown in Fig. 5.

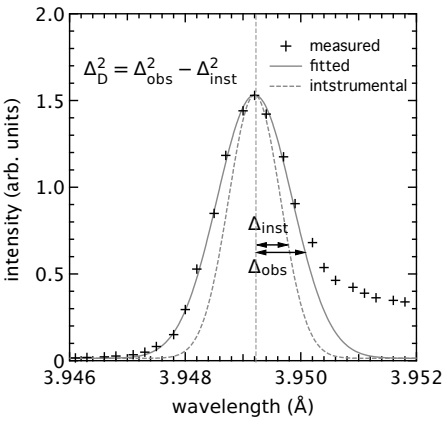

Fig. 7 Measured profile of the w line and instrumental width evaluated at $t = 1.7$ s.

Here, we focus our interest on T_e and T_i derived with argon spectra. Since they are derived from emission lines of the same ion, they should reflect the plasma condition at the same location though the detailed location is unclear. It is observed in Fig. 5 that electrons and ions have yet to reach thermal equipartition before pellet injection. Once n_e is increased, T_i shows the same temporal development with T_e until the end of discharge.

From all these results shown here, one may say that the T_e measurement technique with helium-like ion spectrum has arrived at the level for a practical use as well as the T_i measurement although an attention should be paid to the location where the dominant radiation takes place. This problem can be solved if a higher Z ion is adopted so that the emission is certainly localized at the plasma center.

Acknowledgements

The authors are grateful for the support of LHD experimental group to conduct the experiment in LHD. This study has been made in part under the financial support by the LHD project (NIFS08ULPP527).

[1] S. Morita et al., Rev. Sci. Instrum. **74**, 2375 (2003).
[2] M. Bitter, Phys. Rev. Lett. **43**, 129 (1979).
[3] M. Bitter, Phys. Rev. Lett. **91**, 265001 (2003).
[4] A. H. Gabriel, Mon. Not. R. astr. Soc. **160**, 99 (1972).
[5] O. Marchuk, *PhD thesis* (2004).